TKK Dissertations 193
Espoo 2009

# MATERIAL RELATION TO ASSESS THE CRASHWORTHINESS OF SHIP STRUCTURES

Doctoral Dissertation

**Sören Ehlers**

**Helsinki University of Technology**
**Faculty of Engineering and Architecture**
**Department of Applied Mechanics**

TKK Dissertations 193
Espoo 2009

# MATERIAL RELATION TO ASSESS THE CRASHWORTHINESS OF SHIP STRUCTURES

Doctoral Dissertation

**Sören Ehlers**

Dissertation for the degree of Doctor of Science in Technology to be presented with due permission of the Faculty of Engineering and Architecture for public examination and debate in Auditorium K216 at Helsinki University of Technology (Espoo, Finland) on the 27th of November, 2009, at 12 noon.

**Helsinki University of Technology**
**Faculty of Engineering and Architecture**
**Department of Applied Mechanics**

**Teknillinen korkeakoulu**
**Insinööritieteiden ja arkkitehtuurin tiedekunta**
**Sovelletun mekaniikan laitos**

Distribution:
Helsinki University of Technology
Faculty of Engineering and Architecture
Department of Applied Mechanics
Marine Technology
P.O. Box 5300 (Tietotie 1)
FI - 02015 TKK
FINLAND
URL: http://www.tkk.fi/Units/Ship/index.html
Tel.  +358-9-451 3501
Fax  +358-9-451 4173
E-mail: leila.silonsaari@tkk.fi

ISBN 978-952-248-143-6
ISBN 978-952-248-144-3 (PDF)
ISSN 1795-2239
ISSN 1795-4584 (PDF)
URL: http://lib.tkk.fi/Diss/2009/isbn9789522481443/

TKK-DISS-2667

Multiprint Oy
Espoo 2009

| | |
|---|---|
| ABSTRACT OF DOCTORAL DISSERTATION | HELSINKI UNIVERSITY OF TECHNOLOGY<br>P.O. BOX 1000, FI-02015 TKK<br>http://www.tkk.fi |

Author Sören Ehlers

Name of the dissertation
Material relation to assess the crashworthiness of ship structures

| | |
|---|---|
| Manuscript submitted 24.08.2009 | Manuscript revised 6.10.2009 |
| Date of the defence 27.11.2009 | |
| ☐ Monograph | ☒ Article dissertation (summary + original articles) |

| | |
|---|---|
| Faculty | Faculty of Engineering and Architecture |
| Department | Department of Applied Mechanics |
| Field of research | Naval Architecture |
| Opponent(s) | Professor Jørgen Amdahl |
| Supervisor | Professor Petri Varsta |
| Instructor | Professor Petri Varsta |

**Abstract**

A ship collision accident can result in severe environmental damage and loss of life. Therefore the non-linear finite element method with shell elements is used to assess the crashworthiness of ship steel structures through collision simulations. However, a non-linear finite element-based benchmark revealed inconsistencies and inaccuracies in the results of collision analysis using current material relations and failure criteria. To overcome these problems in this thesis, the steel material's true strain and stress relation is derived in a novel way from tensile experiments until failure on the basis of optical measurements. The novel material relation is obtained until failure with respect to the strain reference length. Furthermore, this material relation, including failure, can be varied to accommodate different finite element sizes. By this means good correspondence in numerical results for the simulation of tensile and plate specimens and complex topologies under indentation loading is achieved for different mesh sizes ranging from 0.88 mm to 140 mm. It is shown that the choice of a constant strain failure criterion suffices for thin steel ship structures. Furthermore, a procedure to optimise a conventional ship side structure for crashworthiness in the conceptual design stage is presented. This procedure extends the assessment procedure for structural arrangements from Germanischer Lloyd. The energy absorbed until inner plate rupture during a right-angle ship collision is used as an optimisation objective. This procedure exploits the novel element length-dependent strain and stress relation, including failure. A particle swarm algorithm is used to identify the crashworthy conceptual design. By this means a crashworthy conceptual ship side structure is obtained, which can absorb significantly more energy than the initial rules-based concept with a reasonable weight increase.

| | | | |
|---|---|---|---|
| Keywords | Ship collision analysis, non-linear FEM, strain and stress relation until failure, optimisation | | |
| ISBN (printed) | 978-952-248-143-6 | ISSN (printed) | 1795-2239 |
| ISBN (pdf) | 978-952-248-144-3 | ISSN (pdf) | 1795-4584 |
| Language | English | Number of pages | 43 + 56 |
| Publisher | Helsinki University of Technology, Department of Applied Mechanics | | |
| Print distribution | Helsinki University of Technology, Department of Applied Mechanics | | |

☒ The dissertation can be read at http://lib.tkk.fi/Diss/2009/isbn9789522481443/

# Preface

This thesis is based on work done at Helsinki University of Technology during 2004–2009. During the thesis process I was financed by the Graduate School of the Helsinki University of Technology, the TÖRMÄKE and SUTERA research projects, and the EU-funded research projects SANDCOR.e, MARSTRUCT, and IMPROVE. This financial help is gratefully acknowledged. Rautaruuki Oy is thanked for providing the test specimen material and Cascade Finland for providing the Aramis license.

I wish to thank my supervisor, Professor Petri Varsta, for his extensive support, encouragement, and valuable discussions during the thesis process. He also provided good working conditions at the Marine Technology Group that enabled me to concentrate on the present investigation.

Special thanks are due to Leila Silonsaari, whose support and help with daily problems is recognised. I would also like to thank Bertil Enquist for providing me with an opportunity to carry out the tensile experiments at Vaxjo University.

I would like to thank my Marine Technology colleagues: Jani Romanoff, Heikki Remes, Alan Klanac, Kristjan Tabri, Jasmin Jelovica, Mikko Jutila, Pentti Kujala, Pentti Tukia, Risto Ripatti, and Seppo Poimuvirta, for their extensive support and helpfulness and for creating a pleasant working atmosphere. I would also like to thank Kari Kantola and Seppo Meriläinen from the Mechanics of Materials Laboratory and Hendrik Naar from Tallinn Technical University for his helpfulness and valuable comments during the thesis process.

Finally, I would like to thank my family and friends and, especially, my wife Ute for their support during the thesis process.

Helsinki, September 2009

Sören Ehlers

# Contents

Appendix

| | |
|---|---|
| [Paper 1] | Ehlers S, Broekhuijsen J, Alsos HS, Biehl F, Tabri K. Simulating the collision response of ship side structures: A failure criteria benchmark study. Int Ship Progress 2008; 55;127-144. |
| [Paper 2] | Ehlers S, Varsta P. Strain and stress relation for non-linear finite element simulations. Thin-Walled Structures 2009, doi:10.106/j.tws.2009.04.005. |
| [Paper 3] | Ehlers S. Strain and stress relation until fracture for finite element simulations of a thin circular plate. Thin-Walled Structures 2009, doi:10.1016/j.tws.2009.08.004. |
| [Paper 4] | Ehlers S. A procedure to optimize ship side structures for crashworthiness. Journal of Engineering for the Maritime Environment 2009, doi:10.1243/14750902JEME179 |

# List of Symbols

| | |
|---|---|
| $A$ | Actual cross-section area of the tensile specimen |
| $A_0$ | Initial cross-section area of the tensile specimen |
| $B$ | Tensile specimen breadth |
| $B1$ | Tensile specimen breadth at clamping location |
| $C$ | RTCL damage model coefficient |
| $D$ | Damage variable |
| $D_{cr}$ | Critical damage variable |
| $D_f$ | Damage variable at failure |
| $\mathbf{F}$ | Deformation gradient tensor |
| $F$ | Force |
| $K$ | Strength coefficient |
| $l$ | Strain reference length |
| $l_e$ | Individual element length |
| $L$ | Tensile specimen length |
| $Lc$ | Clamping length of the tensile specimen |
| $Lm$ | Effective length of the tensile specimen |
| $Lr$ | Tensile specimen transition length between B and B1 |
| $n$ | Strain hardening index |
| $\mathbf{P}_v$ | Coordinates of the deformed points |
| $\mathbf{R}$ | Rotation matrix |
| $t$ | Plate thickness |
| $T$ | Triaxiality |
| $u$ | Displacement |
| $\mathbf{u}$ | Rigid body translations |
| $\mathbf{U}$ | Stretch tensor |
| $\mathrm{d}\mathbf{X}$, $\mathrm{d}\mathbf{x}$ | Line element connecting three facets |
| $x, y, z$ | Global coordinates |
| $x'', y''$ | Tangential plane in x- and y-coordinates |
| $\alpha$ | Factor depending on the necking strain |
| $\gamma$ | Shear angle |
| $\delta l$ | Change in length of $l$ |
| $\varepsilon$ | Strain |
| $\varepsilon_e$ | Necking strain |
| $\varepsilon_E$ | Engineering strain |
| $\varepsilon_f$ | Failure strain |
| $\varepsilon_g$ | Uniform necking strain |
| $\varepsilon_{hyd}$ | Hydrostatic strain |

| | |
|---|---|
| $\varepsilon_m$ | Effective strain |
| $\varepsilon_n$ | Diffuse necking strain |
| $\varepsilon_T$ | True strain |
| $\varepsilon_{1,2,3}^{\mathrm{P}}$ | First, second, and third principle strain |
| $\theta$ | Lode angle |
| $\bar{\theta}$ | Lode parameter |
| $\lambda$ | Eigenvalue |
| $\sigma$ | Stress |
| $\sigma_e, \sigma_{effective}$ | Effective stress |
| $\sigma_E$ | Engineering stress |
| $\sigma_m, \sigma_{hydrostatic}$ | Hydrostatic stress |
| $\sigma_T$ | True stress |
| $\sigma_{1,2,3}$ | First, second, and third principle stress |

## Subscripts

| | |
|---|---|
| $x, y, z$ | $x, y, z$ -directions |
| $xy$ | $xy$ -plane |
| $i$ | Index |

## Abbreviations and Names

| | |
|---|---|
| ARAMIS | Brand name by GOM for their optical measuring system |
| ASIS | Association for Structural Improvement of the Shipbuilding Industry |
| ASM | American Society for Metals |
| Bh | Bulkhead |
| BWH | Bressan-Williams-Hill |
| CB | Coupled Beam |
| E/M | Energy per Mass ratio |
| FEM | Finite Element Method |
| GL | Germanischer Lloyd |
| GLF | Failure criterion according to Germanischer Lloyd |
| GOM | Gesellschaft für Optische Messtechnik |
| MTS | Company name |
| NVA | Norske Veritas Grade A steel |
| PES | Failure criterion according to Peschmann |
| PSO | Particle Swarm Optimisation |
| RAEX | Raahe extra steel from Rautaruukki |
| RTCL | Rice-Tracy and Crockcroft-Latham |
| TNO | Toegepast Natuurwetenschappelijk Onderzoek - Dutch institute for applied physical research |
| udm | user defined material |
| wf | webframe |

# List of Publications and Author's Contribution

This thesis consists of an introductory report and the following four papers:

[Paper 1] Ehlers S, Broekhuijsen J, Alsos HS, Biehl F, Tabri K. Simulating the collision response of ship side structures: A failure criteria benchmark study. Int Ship Progress 2008;55;127-144.

Ehlers prepared the benchmark study and the finite element models and was the main contributor to the manuscript. Broekhuijsen provided the experimental data. Alsos and Biehl carried out the RTCL and PES simulations, respectively. Tabri contributed to the manuscript with valuable comments and suggestions.

[Paper 2] Ehlers S, Varsta P. Strain and stress relation for non-linear finite element simulations. Thin-Walled Structures 2009, doi:10.106/j.tws.2009.04.005

Ehlers carried out the experiments and analysis, performed the validation, and was the main contributor to the manuscript. Varsta contributed to the manuscript with valuable comments and suggestions.

[Paper 3] Ehlers S. Strain and stress relation until fracture for finite element simulations of a thin circular plate. Thin-Walled Structures 2009, doi:10.1016/j.tws.2009.08.004.

Ehlers is the only contributor to this paper.

[Paper 4] Ehlers S. A procedure to optimize ship side structures for crashworthiness. Journal of Engineering for the maritime environment 2009, doi:10.1243/14750902JEME179.

Ehlers is the only contributor to this paper.

# Original Features

The non-linear finite element method with shell elements is used to assess the crashworthiness of ship steel structures through collision simulations. These simulations need to reliably and accurately predict the energy absorbed until fracture for different element sizes. Therefore, a material relation including failure is needed which accounts for the change in element size. Furthermore, to increase the crashworthiness of a conceptual side structure, an evaluation procedure for different scantlings is needed. The following features of this thesis are believed to be original.

1. Non-linear finite element-based benchmarking was carried out to reveal inconsistencies and inaccuracies in the results of collision analysis achieved with different failure criteria using the same material relation and mesh size. The force and penetration predictions for different element sizes using the same material relation and failure criterion do not correspond to each other. [Paper 1]

2. To overcome the inconsistency in collision simulations, the steel material's true strain and stress relation is derived in a novel way from tensile experiments until failure on the basis of optical measurements. The discrete pixel information from the optical measurements serves as the basis on which the strain reference length is clearly defined experimentally. It is shown that the material relation can be defined on the basis of this strain reference length. Furthermore, the strain reference length can be varied. By this means good correspondence in numerical results can be achieved for different mesh sizes ranging from 0.88 mm to 4.4 mm, because the element length is equal to the strain reference length. [Paper 2]

3. The material relation obtained from tensile experiments in Paper 2 is used to simulate a circular plate-punching experiment until fracture. Because of the element length-dependent material relation until failure, the results are in good agreement with the experimental result for different element sizes. [Paper 3]

4. It is shown that a constant strain failure criterion suffices as close triaxiality ranges exist at failure for different tensile specimens. Furthermore, it is shown that the triaxiality at failure is equal for the tensile and plate simulations. The relation between the measured failure strain and the element length is presented. [Papers 2, 3, and 4]

5. The material relation from Papers 2 and 3 is validated for complex structural topologies under indentation loading until fracture on the basis of existing experimental results. Furthermore, this material relation including failure is found to result in a significantly better correspondence of the predicted force and penetration for different element sizes, ranging from 4.4 mm to 140 mm, than present approaches found in the literature and in Paper 1. [Paper 4]

6. To improve the crashworthiness of ship structures, a procedure is presented to include non-linear finite element-based collision simulations into structural optimisation for the conceptual design phase using the novel material relation until failure. A parametric finite element model is built that assigns the material relation and failure strain according to the element size. A particle swarm optimisation algorithm is used to identify the crashworthiness concept. [Paper 4]

# 1 Introduction

## 1.1 Background

A ship collision accident [1, 2] can result in severe environmental damage and loss of life. Looking at the IMO data [3 to 7] shows that the share of collision accidents is about 20% of all serious and very serious accidents. Therefore numerical simulations of such collisions are increasingly being performed to reveal the consequences from a structural point of view. These collision simulations are carried out in a quasi-static fashion for a collision incident, commonly consisting of a ship model that is subjected to a rigid right-angle indenter; see [8]. By this means the deformations of the ship side structure are alone in contributing to the crashworthiness. This allows the structural collision simulation to be uncoupled from the outer dynamics, as this approach results in the maximum energy to be absorbed by a specific structure.

The finite element method is commonly used to carry out the collision simulations, as this numerical method is flexible and widely applicable for complex structures. The reduction of oil spill in tanker collisions was studied by Yamada [9], Urban [10] studied the crushing and fracture behaviour of high-speed craft, and crashworthy ship structures are studied by Törnqvist [11] and Broekhuijsen [12], bulb impacts on large-scale structures by Karlsson [13], and the resistance of bottom structures during stranding by Alsos [14]. These simulations contain highly non-linear structural deformations, including rupture. Therefore, the finite element analyses of ship collision incidents require the input of the true strain and stress relation until failure. In other words, the material relation and a failure criterion to determine the failure strain are needed. Furthermore, the analyses need to be reliable and realistic in order for the crashworthiness of the side structure of the ship to be increased in the conceptual design phase.

In this thesis the term ‘failure strain’ denotes the strain value when fracture occurs, whereas the term ‘failure criterion’ is used to denote the failure of the elements once the failure strain is reached. The term ‘rupture’ is used to describe the existence of fractures in ship structures.

## 1.2 State of the Art

Collision simulations of ship structures are increasingly being performed – see, for example, [11, 13, and 15 to 20] – as experimental testing is unfavourable because of the high cost, the long preparation time, and the need to control large forces; see [21 to 23].

To reduce the computational demand several simplified calculation methods have been developed to assess the energy absorbed during a collision incident. The most famous simplified calculation method was proposed by Minorsky [24]; he was the first to propose splitting the collision process into an external and an internal part. The basic idea is that the energy absorbed is a simple linear function of the volume of deformed material. Furthermore, several simplified calculation methods have been developed to assess the collapse behaviour of predefined structural elements; see, for example, [15, 25 to 32]. These special solutions are known to predict the energy absorption quite accurately. However, the major drawback of simplified analytical methods is their limited validity, which is a consequence of their predefined behaviour. Additionally, their underlying deformation mode assumptions are not necessarily valid for various scantlings.

Therefore, finite element-based analysis of ship collision simulations has been performed in many commercial codes, such as LS-DYNA, ABAQUS, and MSC/DYTRAN, by [33 to 35]. These collision simulations are needed in order to reliably predict the energy to fracture for the conceptual design alternatives. The material's true strain and stress relation is commonly selected in the form of a power law; see, for example, [36 to 42]. The power law parameters can be obtained from standard tensile experiments; see [43 to 47]. However, whether or not the chosen finite element length corresponds to the true strain and stress relation obtained remains questionable. For one selected finite element length, agreement between the numerical simulation and the tensile experiment may be achieved by an iterative procedure. Here the true strain and stress relation, i.e. the power material law, used as input for the simulation is changed until compliance with the corresponding tensile experiment is achieved [37, 38, 41 and 42]. However, this iterative procedure can lead to wrong structural behaviour if the element size is changed, in which case the procedure needs to be repeated for each mesh size selected until compliance is reached. Therefore, the proper material relation until failure is of considerable importance, as it directly influences the accuracy of non-linear finite element simulations until fracture, such as collision simulations.

Furthermore, the determination of the material relation alone does not necessarily suffice, as the failure strain, i.e. the end point of the stress versus strain curve, depends in turn on the material relation. However, a significant amount of research has been conducted to describe criteria to determine the failure strain, for example by [11, 17, 48 to 50], and to present their applicability; see [22, 36, 51 and 52]. However, all of these papers use a standard or modified power law to describe the material behaviour, and none of these papers identifies a clear relation between the true strain and stress relation and the element length. Relations to obtain an element length-dependent failure strain value are given by [11, 12, 17, 48 and 49]. These curve-fitting relations, known as Barba's relations, are obtained on the basis of experimental measurements. However, they define only the end point of the standard or modified power law. This inconsistent adjustment of the element length with respect to the chosen true strain and stress relation can lead to wrong structural behaviour, as no element length dependency of the true strain and stress relation including failure is obtained.

However, qualitative finite element simulations of ship collisions have been used to improve ship side structures through novel crashworthy side structures; see [34, 53 to 55]. So far only Royal Schelde [56] has successfully implemented such novel side structures into inland waterway ships and barges. They followed a procedure similar to the GL assessment procedure for alternative structures [57, 58]. By this means they simulate a collision incident in a quasi-static fashion with a rigid striking bow. A rigid bow results in the absorption of the available energy by the struck ship alone, even though [59, 60] showed that the deformations of the striking bow absorb up to 42% of the available energy. However, with a rigid bow a comparison of different side structures can be made, as the energy absorbed until inner hull fracture is of primary interest for the conceptual design of the side structure. Conventional side structures, however, are usually not optimised for crashworthiness. Klanac et al. [61] presented an optimisation-based procedure to improve the crashworthiness of a conventional ship side structure. However, they use a power law-based material relation including failure and use solely flat bars with a fixed spacing to stiffen the side structure.

## 1.3 Scope of Work

In this thesis, the accuracy of force and penetration predictions from collision simulations for different failure criteria will be presented through a benchmark study. It will be shown that the material relation and failure criteria employed predict the force and penetration inconsistently for different finite element sizes. Therefore, a procedure for the robust crashworthiness assessment of ship structures using the non-linear finite element method will be developed for the conceptual design stage. This crashworthiness assessment will analyse various scantlings for a given collision incident, whereas a collision analysis would simulate a single structural alternative for an incident with one striking location only. Furthermore, this procedure will utilise a particle swarm optimisation algorithm to identify the crashworthy conceptual design alternative. During this optimisation procedure, the energy absorbed until inner plate rupture will be used as an objective. By this means a crashworthy conceptual ship side structure will be obtained, being a light conceptual design that should perform well during a ship collision. The basic requirements of the procedure are:

1. a properly meshed finite element model of the structure to be analysed;
2. because of the discrete nature of the meshed model, an appropriate and thus element length-dependent true strain and stress relation until failure is needed, and
3. the collision analyses must be detailed enough to capture the local behaviour of the structure, yet they have to be fast enough to be implemented into optimisation.

The first requirement means that the meshed finite element model has to be able to undergo major structural deformations caused by the indentation of the rigid bow to predict the force versus penetration curve until inner plate rupture sufficiently well.

The second requirement concentrates on the correct definition of the true strain and stress relation until failure, i.e. the material behaviour. Therefore the true strain and stress relation needs to be sensitive to the chosen element length until failure is reached. Furthermore, it will be shown that this procedure uses the novel element length-dependent true strain and stress relation including failure.

The third requirement indicates that the choice of element size and corresponding material relation has to allow the results of the analyses to have sufficient accuracy for the conceptual design phase. However, the solution time has to remain suitably short in order to allow its implementation into optimisation.

In order to fulfil these criteria, a procedure to determine the true strain and stress relation experimentally until failure on the basis of optical measurements will be given in order to improve the accuracy of the numerical collision simulations. This true strain and stress relation should be suitable for implementation in finite element models as the strain reference length will be clearly defined on the basis of the discrete pixel dimensions from the optical measurements. The influence of the strain reference length, indicated by the letters A and B, on the finite element size and material relation is given in Figure 1. It will be shown that the measured local failure strain serves as a criterion to delete elements to simulate rupture or to terminate the simulation at the point of rupture. Furthermore, this true strain and stress relation until failure will be used to analyse tensile, plate, and complex structural topologies with the finite element method. For validation the results of the analysis will be compared to experimental results and to existing material relations and failure criteria.

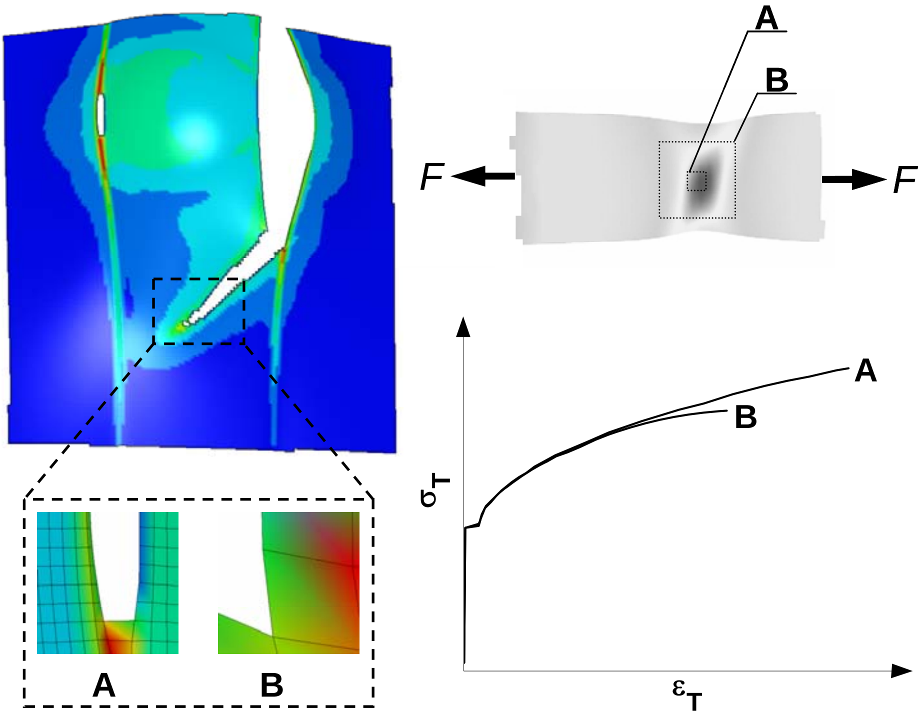

Figure 1: Symbolic element length-dependent true strain and stress relation until failure for numerical collision simulations

## 1.4 Limitations

Ship collision accidents involve a vast number of parameters influencing the consequences of the incident. Therefore, certain limitations are needed to assess the crashworthiness of ship steel structures through collision simulations with the non-linear finite element method. Furthermore, the optimisation for crashworthiness requires the analysis of several thousand individual collision simulations.

Therefore, ship dynamics are excluded from the collision simulations to assess crashworthiness as the energy absorption of the struck ship structure is of primary interest. Therefore, all processes are treated as quasi-static and strain rate effects are not considered.

The striking bow is assumed to be rigid, as only the energy absorption until the rupture of the inner hull of the ship structure is of interest. In this way a direct comparison of different scantlings is possible through their calculated force versus penetration curve until inner hull rupture.

The deformations of the basic plate and stiffener material are of primary interest. Therefore, the material behaviour of the base material is considered by means of the true strain and stress relation and the influence of the welding is not considered. This assumption suffices as stretch deformations occur primarily during the collision simulation.

The accuracy of the collision analysis is applicable for the conceptual design stage. However, a validation with a full-scale collision experiment, performed under laboratory conditions with well-controlled boundaries and deformation measurements, is not possible, as such an experiment does not exist at present.

The optimisation algorithm is used as a tool to improve the conceptual design in each new generation; a possible global optimum from an optimisation point of view is not part of the scope of this thesis.

# 2 Crashworthiness analysis of ship structures

## 2.1 A collision simulation benchmark study [Paper 1]

Numerical collision simulations for three different large-scale structures are carried out with the finite element method with shell elements using LS-DYNA as the solver. A comparison of three different failure criteria is presented, as the same structural models are meshed equally with three different element sizes. Those failure criteria are according to GL [57], Peschmann [49], and Rice-Tracey and Crockcroft-Latham [11, 51]. All three criteria use the same power law material relation. By this means it is shown that the resulting force and penetration predictions do not correspond to each other if different element sizes – 25, 50, and 100 mm – are used for the same failure criterion and material relation. Furthermore, different failure criteria do not behave equally. Hence the choice of an element length-dependent failure strain does not suffice in its present form. Additionally, the power material relation is independent of the finite element size, and has no correspondence to the choice of failure strain determination, i.e. the failure criterion. Therefore, a novel procedure is needed to obtain the material's strain and stress relation including failure with respect to the choice of element size.

## 2.2 Procedure to determine the strain and stress relation [Paper 2]

The common choice of the material's true strain and stress relation in the form of a power law can be obtained from standard tensile experiments; see [43 to 47]. The gauge length for standard tensile experiments depends on the specimen's effective length, or on the choice of extensometer. However, an ideal infinitesimally small gauge length to capture the strain localisation cannot be achieved. Furthermore, no information on the development of the cross-sectional area is obtained during a standard experiment. Therefore, Hoffmann and Vogl [62] traced the development of the cross-sectional area using optical measurements to obtain the strain and stress for a tensile specimen. However, they do not define their gauge length and the corresponding failure strain. Furthermore, the true strain and stress until failure are traced using the finite element method by [37, 43, 44, 46, 62 and 63], but no prediction of the failure strain or the gauge length to capture the localisation is presented. Hogström et al. [64] use optical measurements to obtain the true strain and stress relation on the basis of tensile experiments. However, Hogström et al. focus on the determination of the point of failure for various strain states.

Therefore, the determination of the material relation until failure, i.e. the true strain and stress relation, is shown on the basis of optical measurements, which measure the local displacements on the surface of the specimen. These dog-bone specimens, with different length-to-breadth ratios (L/B), consist of 4-mm-thick NVA and 6-mm-thick RAEX S275 LASER steels. The three tensile specimen types were tested with three specimens each. The displacement-controlled experiments are carried out with a tensile test machine at Växjö University, consisting of a MTS 322 Test Frame with Load Unit. The MTS Test Frame records the force and the resulting elongation of the specimens, in other words the force-elongation curve, which will be used to validate the proposed procedure.

The local strain is calculated from the local displacements obtained by the optical measurements on the basis of a discrete amount of pixel recordings, a so-called facet. The discrete pixel dimensions will clearly define the strain reference length. To determine the stress, the cross-sectional area at any given instant is calculated on the basis of the out-of-plane displacement measurements of the specimen. Therefore the local stress is determined on the basis of the minimum cross-sectional area of the specimen measured as a function of the strain reference length. It has been shown that this stress measure suffices and that corrections for the stress state as introduced by [41, 65] for standard tensile experiments are not needed. The gauge length, i.e. the strain reference length, is shown to be a function of a discrete amount of pixel recordings from the optical measurements. As a result the true strain and stress relation until failure is obtained in a manner that is dependent on the choice of strain reference length. Furthermore, this strain reference length is varied from 0.8 mm to 4.4 mm to show its sensitivity to the true strain and stress relation until failure. As an example the obtained strain and stress relations are shown in Figure 2 for a specimen with a length-to-breadth ratio of 8.

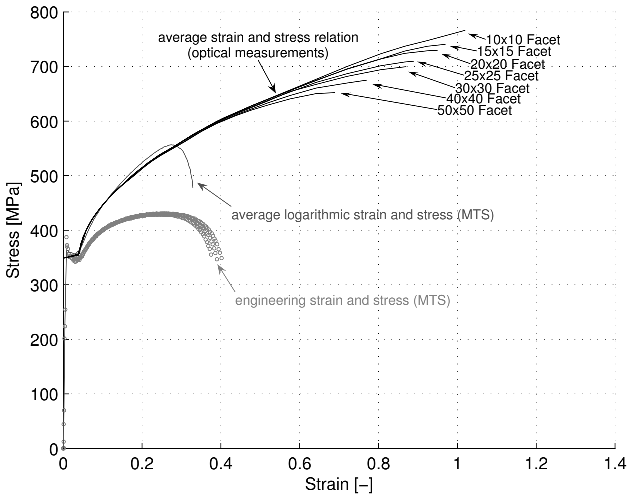

Figure 2: Measured strain and stress relation (MTS measures are plotted for comparison)

## 2.3 Numerical simulations of tensile specimens [Paper 2]

The novel true strain and stress relation until failure obtained with optical measurements is used to simulate a tensile experiment with the finite element method. In this way the proposed material relation is validated, because the numerical results are compared to independently measured force and elongation values from Ehlers and Enquist [66]. The tensile experiments are simulated using the explicit time integration solver LS-DYNA version 971. The structures are modelled using four noded quadrilateral Belytschko-Lin-Tsay shell elements.

The finite element length is equal to the strain reference length. The finite element length ranges from 0.88 mm to 4.4 mm and is equal to the strain reference length for the tensile simulations. Because the optical measurements utilise square-shaped facets, the finite element has to be of a similar square shape. In this way a consistent dependency between the finite element size and the material relation until failure is achieved. The specimen is modelled between the clamping wedges only. The translational degrees of freedom are prohibited at one edge, whereas the other edge is subjected to a constant displacement of 100x the experimental speed as no dynamic effects occur. Additionally, the simulation time remains desirably short. The averaged experimentally determined strain and stress relations are implemented via Material 124 of LS-DYNA. Standard LS-

DYNA hourglass and time step control is used. For details of the modelling and simulation processes see Ehlers et al. [67], Hallquist [68], and Tabri et al. [52].

The initiation and propagation of fracture in the specimens is modelled in LS-DYNA by deleting the failing elements from the model. The element fails once the failure strain is reached. The measured local failure strain serves as a criterion to delete elements to simulate rupture or to terminate the simulation at the point of rupture. The material is assumed to follow the von Mises flow rule, and the element is deleted once the equivalent plastic strain reaches the measured local failure strain. It is shown that the choice of a constant strain failure criterion used for the tensile simulations is justified as close ranges of triaxiality are obtained at the point of failure for specimens with different L/B ratios and thicknesses.

The force versus elongation curves from the tensile experiment simulation correspond to the measurements with good agreement. As an example, the force versus elongation curves that were obtained for a specimen with a length-to-breadth ratio of 8 are shown in Figure 3. The simulation using the element length-dependent true strain and stress relation shows better convergence with changing element lengths, i.e. the strain reference lengths, until the point of failure than the common power law material relation according to ASM [69]; see Figure 3. The resulting element length-dependent true strain and stress relation until failure represents a significant improvement on the existing methods – see, for example, [43 to 47] – used to determine this relation.

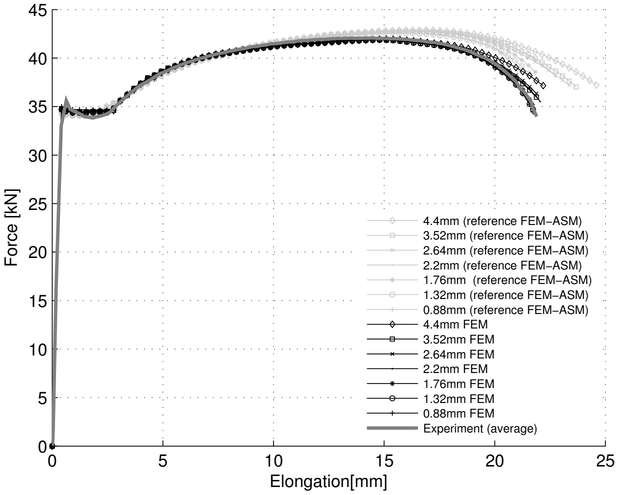

Figure 3: Finite element analysis results

## 2.4 Numerical simulations of plate specimens [Paper 3]

The novel true strain and stress relation until failure obtained with optical measurements is used to simulate a plate-punching experiment with the finite element method. The friction coefficient used in the numerical simulation was estimated to be 0.3. Furthermore, it is shown that this novel true strain and stress relation is sufficiently equal for different specimens, i.e. the L/B ratios. In this way a universal true strain and stress relation until failure is obtained. The proposed material relation is validated for plate deformations until fracture, as the numerical results are compared to the experimental results from [70]. As different strain reference lengths can be used to obtain the novel true strain and stress relation from the optical measurements, different finite element lengths can be employed in the numerical model, these being 0.88, 2.2, and 4.4 mm, as both measurements have to be equal. In this way the same consistent dependency between the finite element size and the material relation until failure is achieved as for the tensile simulations in Paper 2. It is shown that the choice of a constant strain failure criterion used for the plate simulations is justified, as close ranges of triaxiality are obtained at the point of failure. Furthermore, it is shown that the triaxiality at failure is equal for the tensile and plate simulations.

The plate-punching experiment consists of circular specimens with a radius of 170 mm made of the same NVA steel plate as the tensile specimens. The average thickness of the specimens, measured with a calliper prior to the destructive experiment, is 4.12 mm. The specimens are subjected centrally to a hemispherical punch displacing the plate until fracture occurs within the plate field at 2 mm/min. The force and displacement values are recorded during the experiment. The force scatter occurring at a maximum of 0.64 kN or 0.53% is very small. Therefore, the average force-displacement curve is used for comparison to the finite element results. The force-displacement curves show a clear transition from plate bending towards membrane behaviour at a displacement of 2 mm. Prior to fracture the force does not increase as plate thinning, i.e. the necking phenomenon, occurs in a circular pattern at the hemispherical punch. The circular necking of the plate leads to a similar fracture pattern for all specimens; for an example see Figure 4. Fracture occurs very profoundly, causing a large crack in the plate and an immediate drop in the force. An initial loading and unloading test shows a very small amount of plastic deformation during the first cycle, vanishing, however, after the second cycle is applied. Additionally, the bolt holes in the specimens show no signs of deformation for any specimen during the destructive test. All tests are performed in atmospheric conditions at a room temperature of 19.8 °C.

The good correspondence between the numerical and experimental results indicates that the true strain and stress relation is suitable for plate deformation simulations until failure as it describes the non-linear behaviour using different element sizes sufficiently well; see Figure 5. Furthermore, the rupture pattern obtained by the finite element simulation shows good agreement with the experimental observation, especially for the 0.88 mm element length; see Figure 4. This agreement indicates that the procedure used to delete failing elements from the model represents an adequate way to model the fracture propagation.

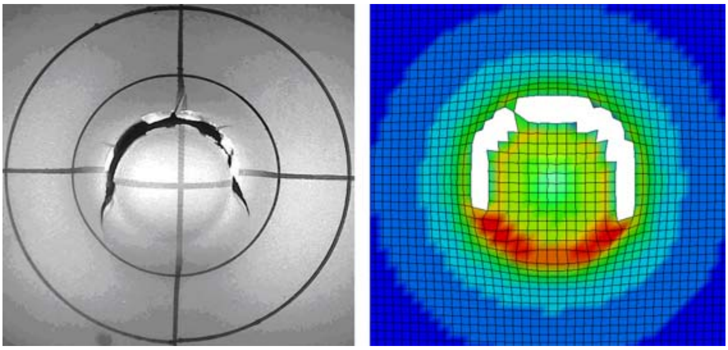

Figure 4: Experimental and numerical rupture pattern of the plate specimen

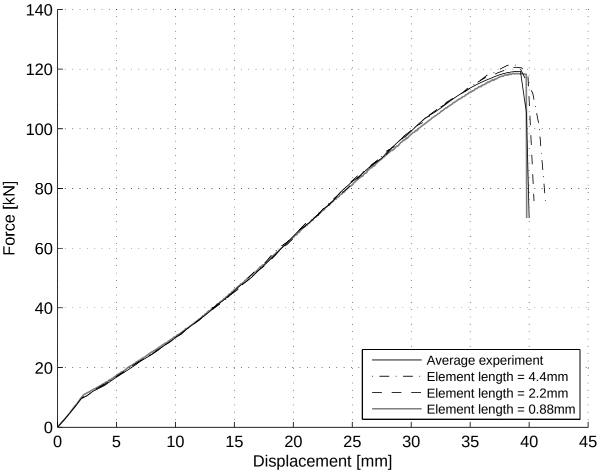

Figure 5: Finite element simulation results for the plate-punching experiment using the element length-dependent strain and stress relation

## 2.5 Numerical simulations of complex structures [Paper 4]

The novel experimentally obtained element length-dependent true strain and stress relation until failure is used to simulate a stiffened plate indentation experiment and a tanker side structure with the finite element method using quadrilateral shell elements. The numerical results for the stiffened plate are compared to existing experimental results from Alsos et al. [36]. In this way the proposed material relation is verified for complex and large-scale structures. Furthermore, the procedure is extended to cover greater element lengths than the strain reference length from the optical measurements. The failure of individual elements is treated in accordance with the findings of Papers 2 and 3. For greater element lengths the true strain and stress relation is found to be independent of the element length, as the extent of the localisation becomes smaller than a single element. However, the element length-dependent failure strain is obtained according to experimental measurements. For small element lengths up to 4.4 mm, the failure strain is obtained with optical measurements, whereas the failure strain for greater element lengths up to 160 mm follows the natural logarithmic form of the well-known engineering strain at failure according to the gauge length of the specimen being 160 mm at a maximum. This failure strain and element length relation allows the removal of failing elements at the correct strain. Furthermore, it is shown on the basis of finite element simulations using shell and solid elements that the failure strain and stress triaxiality do not depend on the plate thickness. Therefore, for thin plates, with a failure mechanism primarily caused by stretching, the triaxiality and the failure strain do not depend on the plate thicknesses.

The resulting force versus penetration curves using different element sizes for the stiffened plate are in good agreement with the existing experimental results from Alsos et al. [36]; see Figure 6. Furthermore, the force versus penetration results from the collision simulation of the tanker structure are in good agreement with each other for different element sizes using the novel material relation and failure strain determination. Additionally, the same collision simulation using an existing power law-based material relation and a failure criterion according to GL [57] results in a significant difference in results for different element sizes.

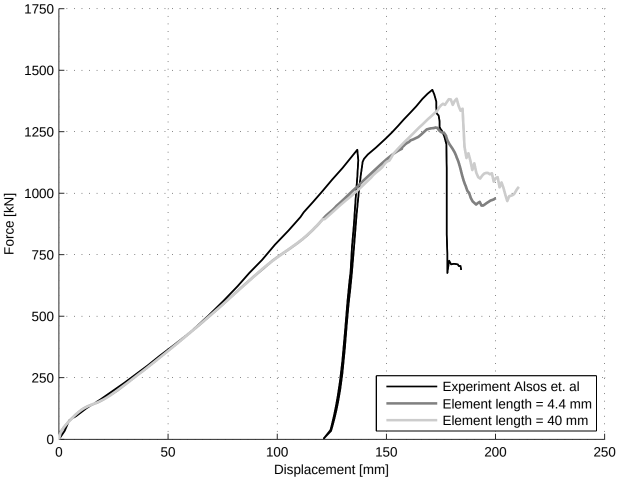

Figure 6: Finite element simulation of a plate stiffened with one flatbar and experimental results by Alsos et al. [36]

## 2.6 Optimisation for crashworthiness [Paper 4]

Optimisation with the objective of increasing the crashworthiness of ship structures has only been performed by Klanac et al. [61] using a genetic algorithm. However, their primary focus is on the relative accuracy of collision simulations, and they do not change the stiffener spacing or type during the collision simulation. Additionally, they carry out collision simulations for one striking location only.

Therefore, this thesis presents a procedure to include non-linear finite element-based collision simulations so as to assess the crashworthiness in optimisation; see, for example, Figure 7. The crashworthiness is assessed for each design alternative on the basis of individual collision simulations for each of four striking locations. Furthermore, each collision simulation is required to be fast in order for the crashworthiness of numerous structural alternatives to be assessed. Therefore, a right-angle collision angle is chosen, because it allows a quasi-static simulation approach. Arbitrary collision angles other than a right angle require the consideration of the outer dynamics of the ship to obtain the energy available for structural deformations and ship motions. However, the solving time for a dynamic ship collision simulation is significantly higher and thus not suitable for optimisation. Furthermore, an arbitrary collision angle would reduce the energy available to deform the conceptual ship structure. Therefore, the optimisation is carried out for this case of maximum available energy for the structural deformations. During the optimisation, the energy absorbed in each simulation until inner plate rupture is calculated and averaged over the four striking locations according to their estimated probability of occurrence. Furthermore, the weight of each design alternative is known. In this way, the energy per mass (E/M) ratio is used as an objective during the optimisation and maximised. The choice of the E/M ratio as the optimality criterion stems from the fact that it combines the structural modifications and the resulting absorbed energy into one criterion. Furthermore, these two individual measures are in conflict with one another. In other words, an ‘ideal’ conceptual design would have zero mass and maximum energy, whereas a minimum mass concept would most probably absorb a small amount of energy, and a maximum energy structure most probably would have a high mass. Therefore, the combination of both criteria results in a structural concept which is the best combination in terms of weight trade-off and absorbed energy, or which is the closest to the ‘ideal’ structure. The optimisation algorithm itself serves as a tool to improve the objective from generation to generation. A particle swarm optimisation (PSO) algorithm – see [71, 72] – is chosen as a tool to identify the crashworthy conceptual design under the defined conditions. The PSO algorithm is written in MATLAB and is based on [73].

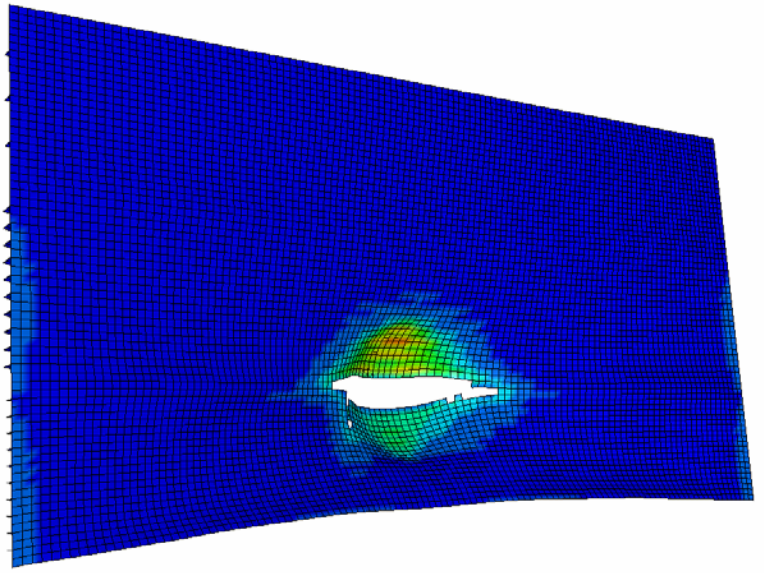

Figure 6: Rupture of the outer plate of the conceptual tanker

Collision simulations carried out within optimisation for crashworthiness need to predict the energy absorbed until inner plate rupture with sufficient accuracy. Therefore the novel true strain and stress relation until failure based on optical measurements is used for the simulations and implemented into the modelling procedure in order to assign the material relation according to the finite element size. The finite element size ranges from 40 mm to 140 mm, depending on the dimensions of the structural members. In order to be able to improve the calculation process, a parametric finite element model is presented. This parametric model is obtained with the ANSYS parametric design language; see Ehlers et al. [74]. It allows the plate thicknesses and the spacing and types of the stiffeners to be adjusted automatically. The explicit non-linear solver LS-DYNA is used for the analysis. MATLAB serves as a control shell to run the optimisation.

As a result a conceptual tanker side structure is optimised for one right-angle collision with four different striking locations. The optimised conceptual design can absorb about 500% more energy than the initial rules-based concept, with a weight trade-off of only 18%. The latter indicates that a simplified approach, such as Minorsky's [24], does not result in a sufficient energy prediction, as the mass distribution between the structural elements of the ship side structure influences the energy absorbed significantly. However, this indicates a significant qualitative trend only, because a direct comparison with the weight increase of the optimised concept does not represent the deformed material alone, as used by Minorsky.

# 3 Discussion

The optimised conceptual design with the highest E/M ratio has a lighter double bottom and deck structure, but a significantly stiffer and heavier side structure. The thickness of the inner bottom is increased slightly, but at the same time the stiffener size is reduced. This increase in thickness is a result of the local strength criteria resulting from the altered structural arrangement. Additionally, the webframe thickness is reduced slightly. Furthermore, the increased stiffness of the side structure will result in even higher energy absorption if the striking bow shape becomes larger, as the contact area increases.

The procedure presented to optimise a ship side structure for crashworthiness requires a consistent material relation until failure. Therefore, the novel material relation developed in Papers 2 and 3 is utilised to predict the energy absorbed until inner plate rupture consistently. Furthermore, it is shown that the power law-based failure criterion according to GL – see [57] – does not predict the energy consistently for different mesh sizes. The latter is essential for the optimisation procedure to guarantee that the optimised structure absorbs more energy than the initial structure. However, the increase in energy can also be obtained by a different choice of steel material, such as austenitic or high-strength steel and aluminium; see, for example, Lehmann and Peschmann [75]. However, the strain and stress relation of these alternative materials is not available in the literature in the proposed form utilised in this thesis.

The assumption that the true stress is obtained as a function of the specimen's cross-sectional area is not entirely correct after localisation occurs. The specimens encounter a stress in the breadth and thickness directions in the necking region, in addition to the longitudinal stress. As a result the effective stress deviates in the necking region from the longitudinal stress, which is, however, used in the finite element simulations presented in this thesis. Additionally, the shell element formulation does not consider stresses in the thickness direction. Therefore only the stress over the specimen's breadth is considered, along with the stress in the longitudinal specimen direction. However, the proposed procedure to obtain an element length-dependent strain and stress relation results in a significantly better force-elongation prediction until the point of failure for the different mesh sizes than the conventional power law fit. This indicates that power law-based material relations do not represent the non-linear material relation sufficiently.

The fracture pattern, i.e. the size of the opening in the side structure of the ship, becomes important if the damage stability or progressive flooding [76] assessment is of interest. Such investigations are being performed in the HASARD project at Chalmers University of Technology [77]. Furthermore, damage assessment after accidental events [78] requires the correct prediction of the size of the opening. However, the crashworthiness assessment procedure presented in this thesis compares different structural arrangements on the basis of the energy absorbed until inner hull rupture. If the fracture pattern is of importance, than an appropriate procedure needs to be identified to compare different fracture patterns. The procedure presented in this thesis can be extended to predict the size of the opening if the energy available for structural deformations is known. The latter can be achieved if the resulting ship motions and their energy consumption are assessed along with the structural deformations during the collision simulation [79]. In other words, the quasi-static optimisation that is presented is a very suitable way to compare the maximum energy absorption capacity of different conceptual structural arrangements as the indentation is stopped as soon as the inner hull ruptures.

The influence of the weld material is not analysed within this thesis. However, the good correspondence of the numerical results – see Paper 3 – and experimental results presented by Alsos et al. [36] indicates that the behaviour of the weld material is sufficiently described by the proposed material relation. Alsos et al. [36] apply a scaling measure for the weld failure to obtain adequate results, but the properties of the weld material are not measured. However, in a large ship structure the majority of the energy will be absorbed by the plate and stiffener deformation, and whether a failing weld results in an increase or decrease in energy will depend on the particular structure.

The influence of the strain rate effect is not considered in the procedure presented in this paper, which is in line with the assumptions presented by [14, 78 and 80]. Furthermore, Alsos et al. [36] present the effect of the strain rate influence on the load increase compared to the fully static scenario as being within a few percentage points. However, they base their findings on the change in global response from two different loading rates of their test structure and they do not study the influence of the strain rate on the material response alone. Therefore, with the target of obtaining a conceptual ship structure which performs well in a collision scenario, this influence can be neglected. Furthermore, a higher strain rate increases the peak load at fracture, so that the structure is able to absorb more energy. Therefore, the quasi-static approach presented in this thesis is on the conservative side, which is, however, beneficial for the conceptual stage of design.

Several studies indicate good correspondence between large-scale collision experiments and numerical simulations using calibrated failure strain values; see, for example, [13, 81 and 82]. Furthermore, good correspondence between experimental and numerical simulations using existing curve fit relations to determine the failure strain has been reported; see, for example, [46, 83 to 85]. However, none of the papers mentioned uses an element length-dependent material relation until failure. Therefore, it remains in question how accurate the given results are, as the vital link between the material relation and the failure strain presented in this thesis is missing.

The decrease in failure strain with increasing element sizes as experimentally confirmed in this thesis is in line with the numerical and experimental findings of [46, 65 and 86]. Furthermore, comparative analysis performed with an arbitrary and a prior chosen failure strain value does not result in reliable conceptual designs as no dependency between the material relation, element size, and failure strain value exists; see, for example, [58, 87 and 88].

# 4 Conclusions

Collision simulations with the non-linear finite element method are presented to assess the crashworthiness of steel ship structures. The accuracy of the force and penetration predictions from collision simulations for different failure criteria existing in the literature is presented through a benchmark study. Insufficient correspondence exists between the force and penetration predictions for different finite element lengths using the current material relations and failure criteria. Therefore a novel finite element length-dependent material relation including failure is presented. A procedure to determine the true strain and stress relation experimentally until failure on the basis of optical measurements is given. The local strain is identified on the basis of the strain reference length. The stress is determined independently of the strain on the basis of the cross-sectional area of the specimen at any given instant as a function of the facet size. The decrease in the reduction of the cross-sectional area with increasing facet size accounts for the averaging of the specimen's cross-section over the extent of the facet size and captures the overall physical behaviour. The finite element simulations are carried out with the finite element length equal to the strain reference lengths. These comparative finite element simulations show very good agreement with the independently recorded force-elongation curve from the MTS Test Frame.

Plate-punching experiments are carried out to verify the applicability of the strain and stress relation obtained from the tensile experiments. This verification is achieved by finite element simulations. These simulations using the strain reference length-dependent and averaged strain and stress relation comply with very good agreement with the average plate-punching experiment. The strain and stress relation that is presented predicts the plate failure sufficiently well. Furthermore, non-linear finite element-based simulations including plate rupture, such as collision simulations, are significantly more accurate if the novel material relation until failure is used. The accuracy and good correspondence of the numerical and experimental results is maintained for different element sizes. Close ranges of triaxiality at failure exist for tensile and plate simulations and the triaxiality at failure is equal for the tensile and plate simulations. Therefore the choice of a constant strain failure criterion suffices for thin steel ship structures, as the deformation is primarily due to stretching.

The results of the visual failure propagation comparison presented in Paper 1 for the failure criteria that were applied show diverse paths, specifically the size of the opening. The latter is important when the damage stability or flooding simulations are of interest. However, the procedure presented in Papers 2 and 3 shows a good correspondence between the experimental fracture pattern and the numerical simulation. This indicates that the future application of the novel material relation can predict the size of the opening sufficiently.

Furthermore, a procedure to optimise a conventional ship side structure for crashworthiness in the conceptual design stage is presented. This is achieved as the energy absorbed until inner plate rupture during a collision is used as an objective during the optimisation procedure. This procedure uses the novel element length-dependent true strain and stress relation including failure. A particle swarm algorithm is used as a tool to increase the crashworthiness of the conceptual design for each new generation. In this way a crashworthy conceptual ship side structure is obtained which can absorb 500% more energy than the initial rules-based concept with a structural mass increase of 18%.

# 5 Future work

The detailed numerical and experimental analysis using the novel element length-dependent material relation until failure and the findings presented in this thesis can improve the accuracy of the non-linear finite element simulations of steel structures. Therefore, this procedure can replace the traditional tensile experiment to determine a strain and stress relation until failure that is suitable for finite element simulations.

The size of the opening after a collision event is becoming more and more important in the context of damage stability analysis. Therefore, the procedure presented here can be combined with the assessment of the motions of the ships during collision simulations. The energy contributing to the structural deformations will be reduced by the energy of the motions of the ships, and thus a realistic opening size remains for the simulated scenario. However, this coupled simulation and determination of the size of the opening requires further validation and analysis to become reliable.

A detailed sensitivity study utilising different material models, including a scatter in material properties or failure criteria would be beneficial in order to further improve the optimisation procedure. Furthermore, this sensitivity study would present convergence to a single optimum conceptual design if the different material models and failure criteria were consistent.

A brief discussion of the strain rate sensitivity is given in this thesis; however, the strain rate is not considered by the proposed procedure to obtain the material relation. A series of additional tensile and plate deformation experiments with different loading rates would outline the sensitivity of the strain rate.

In the future this optimisation procedure can be used to find a minimum weight concept for a certain collision energy if the real scenario and ship types are known. This crashworthy conceptual design can become more realistic if the total cost is assessed during the optimisation and the limits of the production or shipyard technology are considered. Furthermore, the material relation as proposed in this thesis can be obtained for austenitic or high-strength steels and for aluminium. In this way the optimal crashworthy conceptual design can be further improved utilising various materials. Additionally, the proposed procedure can be used to obtain the strain and stress relation of the weld material. Therefore a detailed study of the topic of weld failure could be undertaken in order to improve the understanding of the failure of welded ship structures.

Additionally, if the real operational conditions and stakeholder preferences are known, then this procedure can easily be adjusted to account for various service loads, accident loads, or structural dynamics.

# 6 References

[1] Cahill RA. Collisions and their causes. Third edition, The Nautical Institute, England 2002.

[2] Buzek FJ, Holdert HMC. Collision cases judgments and diagrams. Second Edition, Lloyd’s of London Press, England 1990.

[3] International Maritime Organisation. Casualty statistics and investigations: Very serious and serious casualties for the year 1999. FSI.3/Circ.2, 2001; Available at:http://www.imo.org/includes/blastDataOnly.asp/data_id%3D5397/2.pdf, accessed on: 4 Aug 2008.

[4] International Maritime Organisation. Casualty statistics and investigations: Very serious and serious casualties for the year 2000. FSI.3/Circ.3, 2002; Available at:http://www.imo.org/includes/blastDataOnly.asp/data_id%3D5118/3.pdf, accessed on: 4 Aug 2008.

[5] International Maritime Organisation. Casualty statistics and investigations: Very serious and serious casualties for the year 2001. FSI.3/Circ.4, 2004; Available at:http://www.imo.org/includes/blastDataOnly.asp/data_id%3D8934/4.pdf, accessed on: 4 Aug 2008.

[6] International Maritime Organisation. Casualty statistics and investigations: Very serious and serious casualties for the year 2002. FSI.3/Circ.5, 2005; Available at:http://www.imo.org/includes/blastDataOnly.asp/data_id%3D11539/5.pdf, accessed on: 4 Aug 2008.

[7] International Maritime Organisation. Casualty statistics and investigations: Very serious and serious casualties for the year 2003. FSI.3/Circ.6, 2005; Available at:http://www.imo.org/includes/blastDataOnly.asp/data_id%3D11540/6.pdf, accessed on: 4 Aug 2008.

[8] International ship and offshore structures congress (ISSC). Collision and Grounding, Committee V.1, Vol 2, 2006.

[9] Yamada Y. Bulbous buffer bows: A measure to reduce oil spill to reduce tanker collisions. PhD Dissertation, Department of Naval Architecture and Offshore Engineering, Technical University of Denmark 2006.

[10] Urban J. Crushing and fracture of lightweight structures. PhD Dissertation, Department of Naval Architecture and Offshore Engineering, Technical University of Denmark 2003.

[11] Törnqvist R. Design of crashworthy ship structures. PhD Dissertation, Department of Naval Architecture and Offshore Engineering, Technical University of Denmark 2003.

[12] Broekhuijsen J. Ductile failure and energy absorption of Y-shape test section. Master Thesis, Delft University of Technology, The Netherlands 2003.

[13] Karlsson UB. Structural Integrity Analysis of Critical Elements of RoPax Ships. Doctoral Thesis, Chalmers University of Technology, Göteborg, Sweden 2008.

[14] Alsos HS, Amdahl J. On the resitance of tanker bottom structures during stranding. Marine Structures 2007;20;218-237.

[15] Paik JK, Pedersen PT. Modeling of the internal mechanics in ship collisions. Ocean Engineering 1996;23(2);107-142.

[16] Peschmann J, Kulzep A. Seitenkollision von Doppelhüllenschiffen (Side Collision of Double Hull Ships). Abschlußbericht zum Teil D2A. Hamburg University of Technology 1999.

[17] Scharrer M, Zhang L, Egge ED. Collision calculations in naval design systems, Report. Final report MTK0614 Nr. ESS2002.183, Version 1/2002-11-22, Germanischer Lloyd, Hamburg 2002.

[18] Hong L, Amdahl J. Strength Design of FPSOs against Supply Vessel Bow Collision. In Proceedings of the Fourth International Conference on Collision and Grounding of Ships, Germany 2007;1-10.

[19] Tavakoli MT, Amdahl J, Alsos HS, Klæbo F. Analysis of supply vessel stern impacts with FPSO. In Proceedings of the Fourth International Conference on Collision and Grounding of Ships, Germany 2007;19-28.

[20] Biehl F, Lehmann E. Collision of Ships with Offshore Wind Turbines: Calculation and Risk Evaluation. In Proceedings of the Fourth International Conference on Collision and Grounding of Ships, Germany 2007;55-61.

[21] Kitamura O, Kuroiwa T. A study on the improved tanker structure against collision and grounding damage. Proceedings of the Seventh International Symposium on Practical Design of Ships and Mobile Units (PRADS), Elsevier B.B., The Hague, The Netherlands 1998;173-179.

[22] Peschmann J, Kulzep A, Lehmann E. Structural behaviour of double-hull ships in collision and grounding. Ship Technology Research 2002;49.

[23] Endo H, Yamada Y, Kitamura O, Suzuki K. Model test on the collapse strength of the buffer bow structures. Marine Structures 2002;15;365-381.

[24] Minorsky VU. An analysis of ship collision with reference to protection of nuclear power plants. Journal of Ship Research 1959;1-4.

[25] Pedersen P, Zhang S. Absorbed Energy in Ship Collisions and Grounding; Journal of Ship Research 2000;44;2.

[26] Wierzbicki T, Abramowicz W. On the Crushing Mechanics of Thin-walled Structures; Journal of Applied Mechanics 1983;50.

[27] Abramowicz W. Crush Resistance of `T´, `Y´ and `X´ Sections; Technical Report 24, Joint MIT – Industry Program on Tanker Safety 1994.

[28] Amdahl J. Energy Absorption in Ship – Platform Impact; Ph.D. thesis, Department of Marine Technology, Norwegian Institute of Technology 1982.

[29] Ueda Y, Rashed SMH, Abdel-Nasser Y. An improved ISUM rectangular plate element taking account of post-ultimate strength behaviour; Marine Structures 1994;7(2-5);139-172.

[30] Paik JK, Seo JK. A method for progressive structural crashworthiness analysis under collisions and grounding. Thin-Walled Structures 2007;45;15–23.

[31] Hong L, Amdahl J. Crushing resistance of web girders in ship collision and grounding. Marine Structures 2008;21;374-401.

[32] Yamada Y, Pedersen PT. A benchmark study of procedures for analysis of axial crushing of bulbous bows. Marine Structures 2008;21(2-3);257-293.

[33] Kitamura O. Comparative Study on Collision Resistance of Side Structure; International Conference on Design and Methodologies for Collision and Grounding Protection of Ships, San Francisco, California, USA, August 22-23, 1996. Also in Marine Technology, Vol. 34, No. 4, 293-308.

[34] Sano A, Muragishi O, Yoshikawa T. Strength Analysis of a New Double Hull Structure for VLCC in Collision; International Conference on Design and Methodologies for Collision and Grounding Protection of Ships, San Francisco, California, USA, August 22-23, 1996.

[35] Kuroiwa T. Numerical Simulation of Actual Collision & Grounding Accidents; International Conference on Design and Methodologies for Collision and Grounding Protection of Ships, San Francisco, California, USA, August 22-23, 1996.

[36] Alsos HS, Amdahl J, Hopperstad OS. On the resistance to penetration of stiffened plates, Part II: Numerical analysis. International Journal of Impact Engineering 2009;36;875-887.

[37] Huatao J, Roehr U. Investigations of Rupture Failure of Welding Line. In Proceedings of the Third International Conference on Collision and Grounding of Ships, Japan 2004;268-275.

[38] Isselin J, Lost A, Golel J, Najjar D, Bigerelle M. Assessment of the constitutive law by inverse methodology: small punch test and hardness. Journal of Nuclear Materials 2006;352(1-3);97-106.

[39] Lee YW, Woertz JF, Wierzbicki T. Fracture prediction of thin plates under hemi-spherical punch with calibration and experimental verification. International Journal of Mechanical Sciences 2004;46;751-781.

[40] Simonsen BC, Lauridsen LP. Energy absorption and ductile failure in metal sheets under lateral indentation by a sphere. International Journal of Impact Engineering 2000;24;1017-1039.

[41] Zhang KS. Fracture prediction and necking analysis. Engineering Fracture Mechanics 1995;52(3);575-582.

[42] Zhang ZL, Hauge M, Ødegård J, Thaulow C. Determining material true stress-strain curve from tensile specimens with rectangular cross-section. International Journal of Solids and Structures 1999;36(23);3497-3516.

[43] Joun MS, Eom JG, Lee MC. A new method for acquiring true stress-strain curves over a large range of strains using a tensile test and finite element method. Mechanics of Materials 2008;40;586-593.

[44] Koc P, Stok B. Computer-aided identification of the yield curve of a sheet metal after onset of necking. Computational Materials Science 2004;31(1-2);155-168.

[45] Mirone G. A new model for the elastoplastic characterization and the stress-strain determination on the necking section of a tensile specimen. International Journal of Solids and Structures 2004;41(13);3545-3565.

[46] Paik JK. Practical techniques for finite element modelling to simulate structural crashworthiness in ship collision and grounding (Part I: Theory). Ships and Offshore Structures 2007;2:1;69-80.

[47] Springmann M, Kuna M. Identification of material parameters of the Gurson-Tvergaard-Needleman model by combined experimental and numerical techniques. Computational Materials Science 2005;32(3-4);544-552.

[48] Alsos HS, Hopperstad OS, Törnqvist R, Amdahl J. Analytical and numerical analysis of local necking using a stress based instability criterion. International Journal of Solids and Structures 2008;45;2042-2055.

[49] Peschmann J. Energy absorption computations of ship steel structures under collision and grounding (translated from German). Doctoral Dissertation. Technical University of Hamburg 2001.

[50] Servis D, Samuelides M. Implementation of the T-failure criterion in finite element methodologies. Computers and Structures 2006;84;196–214.

[51] Törnqvist R, Simonsen BC. Experimental and numerical modeling of ductile crack propagation in large-scale shell structures. Marine Structures 2004;17;1-27.

[52] Tabri K, Alsos H, Broekhuijsen J, Ehlers S. A benchmark study on ductile failure criteria for shell elements in multiaxial stress state. In Proceedings of the first International Conference on Marine Structures, Marstruct, Glasgow, United Kingdom 2007;401-409.

[53] Ehlers S, Klanac A, Tabri K. Increased safety of a tanker and a RO-PAX vessel by implementing a novel sandwich structure. In Proceedings of the Fourth International Conference on Collision and Grounding of Ships. Germany 2007;109-115.

[54] Klanac A, Ehlers S, Tabri K, Rudan S, Broekhuijsen J. Qualitative design assessment of crashworthy structures. In Proceedings of the International Maritime Association of Mediterranean, Portugal 2005;461-469.

[55] Konter A, Broekhuijsen J, Vredeveldt A. A quantitative assessment of the factors contributing to the accuracy of ship collision predictions with the finite element method. In Proceedings of the Third International Conference on Collision and Grounding of Ships. Japan 2004;17-26.

[56] van de Graaf B, Broekhuijsen J, Vredeveldt A. Construction aspects for the Schelde Y-shape crashworthy hull structure. In Proceedings of the Third International Conference on Collision and Grounding of Ships, Japan 2004;229-233.

[57] Zhang L, Egge ED, Bruhms H. Approval procedure concept for alternative arrangements. In Proceedings of the Third International Conference on Collision and Grounding of Ships, Japan 2004;87-97.

[58] Ozguc O, Das PK, Barltrop N. A comparative study on the structural integrity of single and double side skin bulk carriers under collision damage. Marine Structures 2005;18;511-547.

[59] Reckling KA. Mechanics of Minor Ship Collisions; International Journal of Impact Engineering 1983;1(3);281-299.

[60] Lehmann E, Yu X. On ductile rupture criteria for structural tear in the case of ship collision and grounding. Practical Design of Ships and Mobile Units (PRADS), Elsevier B.B., The Hague, The Netherlands 1998;149-156.

[61] Klanac A, Ehlers S, Jelovica J. Optimization of crashworthy marine structures. Marine Structures 2009;1-21.

[62] Hoffmann H, Vogl C. Determination of True Stress-Strain-Curves and Normal Anisotropy Tensile Tests with Optical Strain Measurement. CIRP Annals - Manufacturing Technology 2003;52(1);217-220.

[63] Ling Z. Uniaxial True Stress-Strain after Necking. AMP Journal of Technology. 1996;5;37-48.

[64] Hogström P, Ringsberg JW, Johnson E. An experimental and numerical study of the effects of length scale and strain state on the necking and fracture behaviours in sheet metals. International Journal of Impact Engineering 2009;36;1194-1203.

[65] Mirone G. Elastoplastic characterization and damage predictions under evolving local triaxiality: axisymmetric and thick plate specimens. Mechanics of Materials 2008;40;685-694.

[66] Ehlers S, Enquist B. Uniaxial tensile necking of steel dog-bone specimens. Helsinki University of Technology, Ship Laboratory 2007;M-303.

[67] Ehlers S, Tabri K, Schillo N, Ranta J. Implementation of a novel ship side structure into a tanker and a ropax vessel for increased crashworthiness. 6th European LS-DYNA Users' Conference, Gothenburg, Sweden 2007, 4.111-4.120.

[68] Hallquist JO. LS-DYNA Theory Manual. Livermore Software Technology Corporation. 2005.

[69] ASM Handbook. Mechanical Testing and Evaluation. 2000;8.

[70] Ehlers S. A thin circular plate under hemi-spherical punch, an experimental study of a plate subjected to a displacement controlled punch. Helsinki University of Technology 2009; Series AM-7.

[71] Eberhart RC, Kennedy J. A new optimizer using particle swarm theory. In Proceedings of the Sixth International Symposium on Micromachine and Human Science, Nagoya, Japan 1995;39-43.

[72] Kennedy J, Eberhart RC. Particle swarm optimization. In Proceedings of IEEE International Conference on Neural Networks, Piscataway, NJ. 1995;1942-1948.

[73] Jalkanen J. Particle swarm optimization of load carrying structures. Journal of Structural Mechanics 2006;2;23-35.

[74] Ehlers S, Klanac A, Kõrgesaar M. A design procedure for structures against impact loading. STG Yearbook 2008, in press.

[75] Lehmann E, Peschmann J. Energy absorption by the steel structure of ships in the event of collision. Marine Structures 2002;15;429-441.

[76] Ruponen P. Progressive flooding of a damaged passenger ship. Doctoral dissertation, Helsinki University of Technology 2007.

[77] HASARD: Holistic Assessment of Ship Survivability and Risk after Damage. Research Project at the Department of Shipping and Marine Technology, Chalmers University of Technology.

[78] International ship and offshore structures congress (ISSC). Damage assessment after accidental events, Committee V.1, Vol 2, 2009.

[79] Pill I, Tabri K. Finite element simulations of ship collisions: A coupled approach to external dynamics and inner mechanics. In Proceedings of the second International Conference on Marine Structures, Marstruct, Portugal 2009.

[80] Wang G, Arita K, Liu D. Behavior of a double hull in a variety of stranding or collision scenarios. Marine Structures 2000;13;147-187.

[81] Naar H, Kujala P, Simonsen BC, Ludolphy H. Comparison of the crashworthiness of various bottom and side structures. Marine Structures 2002;15;443-460.

[82] Servis D, Samuelides M, Louka T, Voudouris G. Implementation of Finite-Element Codes for the Simulation of Ship-Ship Collisions. Journal of Ship Research 2002;46(4);239-247.

[83] Paik JK. Practical techniques for finite element modelling to simulate structural crashworthiness in ship collisions (Part II: Verification). Ships and Offshore Structures 2007;2(1);81-85.

[84] Lehman E, Yu X. Progressive Folding of Bulbous Bows; in the Sixth International Symposium on Practical Design of Ships and Mobile Units (PRADS) 1995.

[85] Samuelides MS, Voudouris G, Toulios M, Amdahl J, Dow R. Simulation of the behaviour of double bottoms subjected to grounding actions. In Proceedings of the Fourth International Conference on Collision and Grounding of Ships, Germany 2007;93-102.

[86] Darie I, Lehmann E. Damage evaluation of bow structures of a Ro-Ro ferry in case of collision. In Proceedings of the Fourth International Conference on Collision and Grounding of Ships, Germany 2007;243-250.

[87] Li NY, Karr DG, Wang G. Mesh size effects in simulating ductile fracture of metals. In Proceedings of 10th International Symposium on Practical Design on Ships and Other Floating Structures. Houston, Texas United States of America 2007:247-254.

[88] Huato J, Yongning Gu. Study on Ship Collision and Buffer Bow Structures. In Proceedings of the Third International Conference on Collision and Grounding of Ships, Japan 2004;172-181.

[89] Takaoka Y, Shimoda T, Yagi S, Kumamoto H, Muragishi O, Törnqvist R, Kennedy SJ, Brooking M. A study on buffer bow design for SEA-Arrow. In Proceedings of the Third International Conference on Collision and Grounding of Ships, Japan 2004;188-194.

ISBN 978-952-248-143-6
ISBN 978-952-248-144-3 (PDF)
ISSN 1795-2239
ISSN 1795-4584 (PDF)